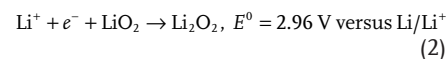
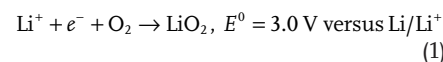


Wetting Behavior of Aprotic Li–Air Battery Electrolytes

Alexander Kube,* Fabian Bienen, Norbert Wagner, and Kaspar Andreas Friedrich

The open architecture of cathodes in Li–air batteries implies the need for open porosity with adequate pore size distribution and surface energy optimization with regard to the electrolyte. The interaction of liquid and cathode material, especially the wetting properties, which depend on cathode material, roughness and porosity, and electrolyte properties, needs to be understood properly to avoid flooding and assure high active areas. In this work, contact angle goniometry, capillary rise method, and pressure saturation curves are used to investigate the wetting properties of dimethyl sulfoxide (DMSO), tetraethylene glycol dimethyl ether (Tetraglyme), a 1:1 mixture of ethylene carbonate and dimethyl carbonate (EC:DMC) and water on a gas diffusion layer (GDL) Sigracet 39BC, and a pure flat polytetrafluorethylene (PTFE) foil. Contact angle measurement shows that all three organic solvents wet the GDL hydrophobic agent PTFE. Capillary rise measurements show that all sample liquids slowly imbibe into the porous network. While for Tetraglyme an efficient penetration is limited by the high viscosity, water flow rate is slowed down by the hydrophobic pore network of the GDL. Pressure saturation curves for DMSO, Tetraglyme, and EC:DMC can be obtained for the first time and are compared with the water pressure saturation curve.



The necessary connection of the cathode to air via an open cell design is associated with development challenges. First, Li metal is explosively reactive with water, and thus a nonaqueous electrolyte is required. In addition, humidity needs to be avoided by air permeable but water-repellant membranes and water free electrolytes on anode side. Therefore, most research is done on completely nonaqueous systems, where the organic electrolyte is used on the anode and cathode side. However, organic electrolytes face challenges of its own. Since most gas diffusion electrodes (GDEs) are optimized for water-based electrolytes with polytetrafluoroethylene (PTFE) as nonwetting/hydrophobic binder an understanding how organic electrolytes interact with these

GDEs is necessary. The nonwetted areas inside the porous system are essential to provide multiple three-phase contact points where gas, electrolyte and active materials are present. The liquid covers the active area with a thin film ensuring the ionic transport to the active sites, while the nonwetted regions ensure proper gas transport to the active areas.


Figure 1 shows a schematic view of a water-based electrolyte film near PTFE and how the current density is linked to the liquid film thickness on the electrode surface. Near the PTFE only a thin liquid film is formed hindering ionic transport (orange region). On the other side with thick electrolyte layers or even flooded pores the diffusion of oxygen to the active side is hindered by long diffusion paths (yellow region). The slow oxygen diffusion in liquids results in increased concentration overpotentials. In between these two regions the optimal balance between ionic transport and oxygen diffusion length gives the maximum current density (green region). If electrolytes with superior wetting properties are used, the three-phase regions in the green region are reduced and the porous system exhibits lower electrochemical performance. Eventually a completely flooded electrode where nearly all active sites are covered with liquid results in inferior performance.^[2] This problem occurs especially for organic liquids with low surface tension.^[3] The influence of slowly increasing electrolyte penetration was investigated by Wagner et al. for alkaline fuel cells, where they observed decomposition of PTFE and therefore a loss of hydrophobic areas inside the porous system. This reduced the thickness of the three-phase boundary with a loss of electrochemical performance of 12–15% after 5000 h

1. Introduction

Li–air batteries have drawn much attention over the last years as energy storage devices for electric vehicles and grid storage because of their potentially high energy density; which theoretically can be up to five times larger than of conventional Li-ion batteries. This high energy density is due to the fact that the cathode reactant is not stored inside the battery. Two principally different approaches for electrolytes on the cathode side are used, namely water-based electrolytes and as second approach organic electrolytes. The following reactions occur at the cathode while discharging the battery in organic electrolyte^[1]

A. Kube, F. Bienen, N. Wagner, K. A. Friedrich
German Aerospace Center
Pfaffenwaldring 38–40, 70569 Stuttgart, Germany
E-mail: alexander.kube@dlr.de

K. A. Friedrich
Institute of Building Energetics
Thermal Engineering and Energy Storage (IGTE)
University of Stuttgart
Pfaffenwaldring 31, 70569 Stuttgart, Germany

 The ORCID identification number(s) for the author(s) of this article can be found under <https://doi.org/10.1002/admi.202101569>.

© 2021 The Authors. Advanced Materials Interfaces published by Wiley-VCH GmbH. This is an open access article under the terms of the Creative Commons Attribution License, which permits use, distribution and reproduction in any medium, provided the original work is properly cited.

DOI: 10.1002/admi.202101569

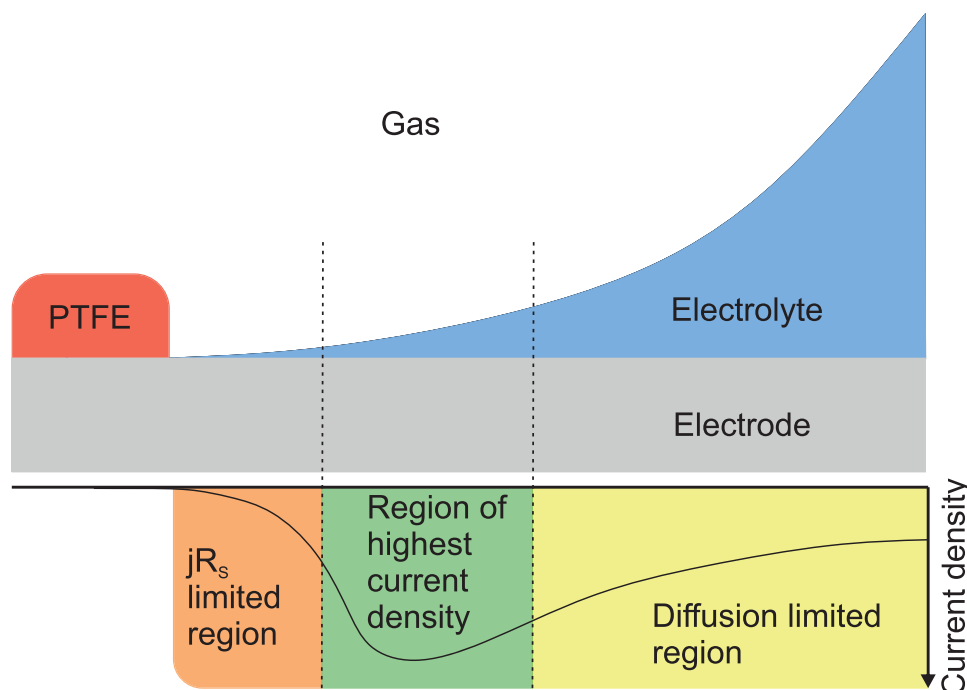


Figure 1. Schematic view of a water-based electrolyte film near PTFE and the correlation of the liquid film thickness to the current density.

operation.^[4] For Li–air batteries little work has been done to investigate the wetting properties so far. Xia et al. produced a partially wetted cathode by evaporation of diethyl ether from the organic electrolyte and showed increased reaction kinetics,^[5] while Andrei et al. showed a dependence of the oxygen diffusion length on the specific capacity,^[6] indicating that controlling the wetting of the porous network leads to higher capacities and rate capabilities. This correlation between oxygen diffusion length and capacity is believed to be due to the precipitation of Li_2O_2 at regions with high oxygen saturation, e.g., near the gaseous supply chamber, resulting in a blockage of oxygen diffusion paths into the porous network.^[7]

If electrodes are not optimized for the used electrolyte, the electrode performance remains inferior since the active area is underutilized. In particular a complete flooding of the porous system is to be avoided as it yields a blockage of the reactant gases/oxygen to the reaction sites, which limits the current and raises the overpotential. The understanding of the wetting behavior of the porous system for the used electrolytes is of crucial importance for high cycle life and low over potentials during charge and discharge of the battery. The key to this problem is the surface energy of the liquid and solid interface as it determines the electrolyte distribution inside the GDE. For water-based electrolytes PTFE is used to determine the hydrophobic properties of the GDE and water film free areas, which is why we first investigate the wetting properties of water on a PTFE foil by contact angle measurements. Relevant aprotic solvents, namely, tetraethylene glycol dimethyl ether (Tetraglyme), dimethyl sulfoxide (DMSO), and a 1:1 mixture of ethylene carbonate and dimethyl carbonate (EC:DMC), were studied with the same procedure. In a second approach, we measure the contact angle over time on our porous sample to characterize the penetration of electrolyte into the porous system. The penetration behavior was then further investigated by a capillary rise experiment.

Capillary rise experiments describe the time dependence of the height rise of a liquid column inside a porous system in contact with a sample liquid and is used to determine the contact angle inside the porous system.^[8–10] Furthermore, it provides data to analyze the wetting kinetics and determine wetting rates.^[11] We could show that all organic solvents intruded the porous system but the intrusion time depended on the contact angle of the solvent on PTFE as well as of the viscosity. As a third characterization technique we used capillary pressure measurements as these can resolve the influence of the microstructure inside the sample. Unlike in the reported setups,^[12–14] where this technique was used to characterize influences of surface modifications and varied amounts of the nonwetting agent PTFE in fuel cells with solely water as test liquid we developed an omniphobic membrane to allow for the measurement of organic solvents with low polarity. This work focuses on influences of different wetting behavior of the used liquids and for the first time shows pressure saturation curves for DMSO, Tetraglyme, and EC:DMC. Such measurements are also crucial for developing and validation of models to describe transport and electrolyte penetration. Pressure saturation curves are often solely calculated by models and validation with experimental data is rare. This is why the measurements conducted in this work are an important part for further development of the models and therefore further development of Li–air batteries and other GDEs using aprotic solvents.

2. Results

2.1. Contact Angle Measurement

Wettability of liquids on flat surfaces is measured by the equilibrium contact angle θ between the liquid-and-solid phase.

The contact angle is determined by the energetic minimum between the solid, liquid and gas phase and can be expressed by Young's equation

$$\gamma_{SV} - \gamma_{SL} = \gamma_{LV} \cos(\theta) \quad (3)$$

With the surface energy γ between solid and vapor (SV), solid and liquid (SL), and between liquid and vapor (LV). The wetting depends on the surface energy balance of all three phases,^[15] where contact angles above 115° indicate a highly nonwetting liquid, contact angles below 65° indicate a highly wetting liquid. Contact angles between 65° and 115° indicate an intermediate wettability of the liquid. Superior GDE performance is achieved in the nonwetting regime. If a liquid is in the wetting regime, imbibed liquid in the porous structure will spread and eventually block gas diffusion to the active sites. Measured wettability for a porous structure is always a mixed wettability from all contact angles of the solid porous network. Additionally, the roughness and porosity do also affect the wetting behavior. GDEs for water-based electrolytes consist of PTFE as nonwetting solid and a supported catalyst with adequate wettability and conductivity; often carbon supports are used. Wettability of water on carbon is based on the carbon type,^[16] for example graphite has a reported contact angle of 86° for water^[17] which is more likely to be wetted than graphene with a contact angle of 127°.^[18] All together the mixture of different materials inside a GDE results in a mixed average wettability.^[19]

For water-based electrolytes, PTFE is used as a binder and to adjust the hydrophobicity. **Figure 2** shows droplets of a) H₂O, b) EC:DMC, c) DMSO, and d) Tetraglyme on a PTFE foil. While H₂O shows a slightly nonwetting behavior (109.05° ± 0.15°), which is reported by many other studies,^[20,21] DMSO shows a mildly wetting behavior (75.40° ± 1.00°) which is comparable to contact angle of 80° of DMSO on FEP.^[22] Both EC:DMC (61.85° ± 0.65°) and Tetraglyme (62.95° ± 0.35°) show an advanced wetting of PTFE. During battery cycling the high wetting corresponds to an undefined triple phase boundary in an actual electrode and furthermore, during discharge Li₂O₂ is

precipitated into the porous electrode, pushing the electrolyte further into the gas diffusion layer (GDL). Both effects favor a high saturation level of liquid inside the porous system, limiting the rate capability and capacity. Due to the wetting nature of the organic solvents on PTFE, electrolyte is imbibed in the porous system in each discharge cycle. If no external gas pressure is applied, the feed gas has to work against the strong wetting force leading to a flooded electrode. Eventually the flooding can lead to cell failure either due to a dry out of the anode and/or breakthrough of electrolyte into the gas chamber.

It is known that the surface structure can strongly influence the wetting behavior. For example, if liquid is placed onto a porous media, it will either show a bridging type drop with nonwetting behavior or it will fill the porous system with liquid. The former is often named "lotus leaf" effect, where water drops on rough surfaces are stabilized by the surface energy. Two approaches to describe these phenomena are commonly used in literature. If the liquid imbibes into the pores of a solid with surface roughness the Wenzel expression with the surface roughness factor r , is applied to the measured contact angle Θ_w to obtain the apparent contact angle Θ^{23}

$$\cos(\Theta_w) = r \cos(\Theta) \quad (4)$$

This is also called homogenous wetting regime, since the liquid completely penetrates into the grooves of the rough surface.

If the liquid does not penetrate into the porous or rough structures the Cassie-Baxter correlation is applied, which results in a heterogeneous wetting regime. This heterogeneous regime is due to the partially wetting of the surface by the liquid phase, while the rest of the surface is wetted by the gas phase^[24]

$$\cos(\Theta_{CB}) = f_s \cos(\Theta_s) + (1 - f_s) \cos(\Theta_{air}) \quad (5)$$

With the fractional area f of the solid in contact with the base of the liquid drop and $(1 - f)$ the remaining fraction of the drop base, the contact angle Θ_s on a flat smooth solid surface, having

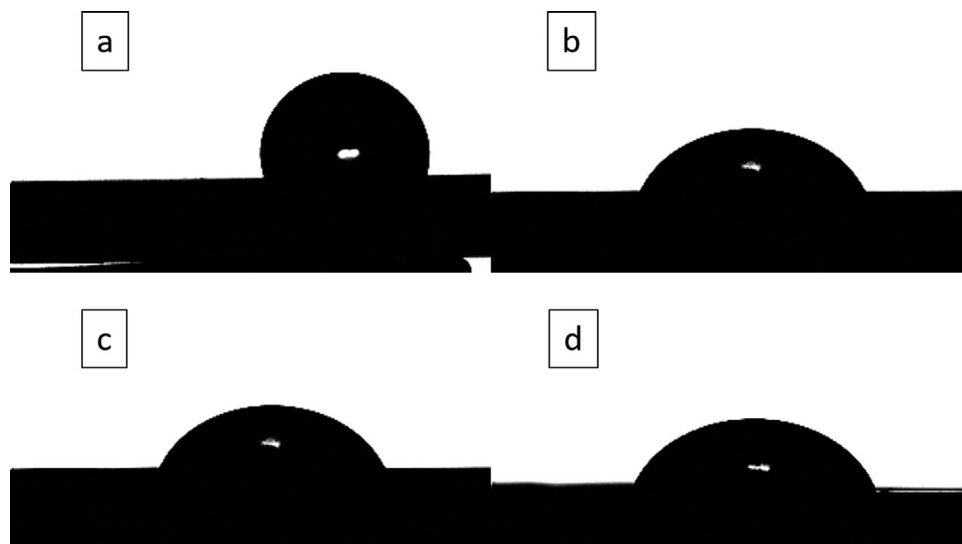


Figure 2. Contact angles of a 15 µL drop of a) H₂O, b) EC:DMC, c) DMSO, and d) Tetraglyme on a flat smooth PTFE foil.

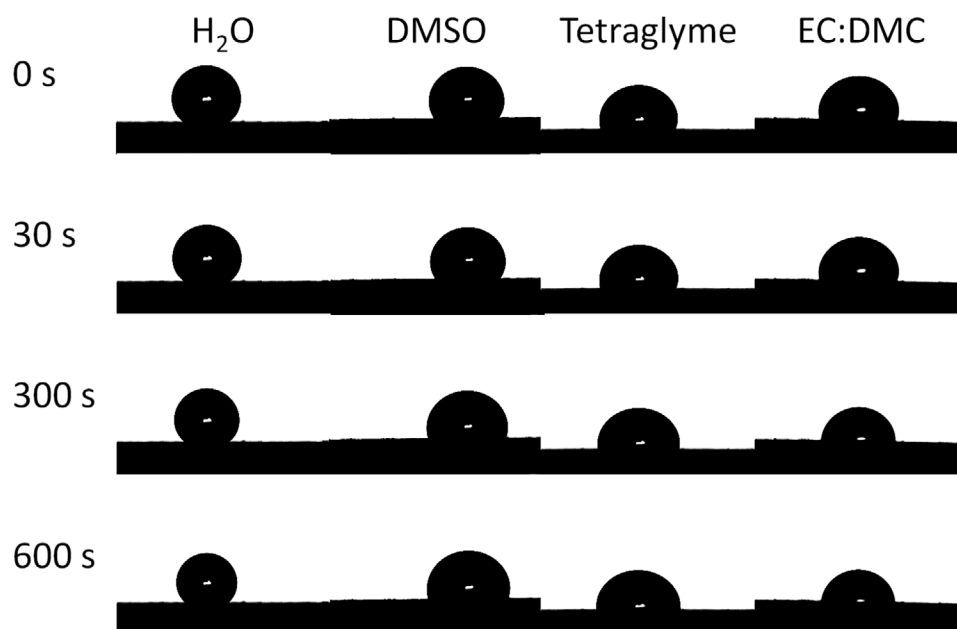


Figure 3. Contact angle time series of a 15 μL drop of H_2O , DMSO, Tetraglyme, and EC:DMC on a GDL 39BC.

the same chemistry as the rough surface, and the contact angle Θ_{air} formed by the liquid in air, which normally is 180° .

The roughness in a homogeneous wetting regime leads to an increase in the wetting or nonwetting behavior. For contact angles above 90° , measured on a flat smooth surface, the contact angle becomes larger for rough samples. For contact angles below 90° , the observed contact angles become smaller. While in the case of heterogeneous wetting, the observed contact angle always appears larger.

Figure 3 shows contact angle measurements on a GDL Sigracet 39BC and **Table 1** the evaluated contact angles from the corresponding images. For pictures taken at 0 s the same trend for contact angles as for a flat surface can be seen, with H_2O as the sample liquid with the highest contact angle of $139.65^\circ \pm 0.35^\circ$, EC:DMC ($105.15^\circ \pm 4.05^\circ$) and Tetraglyme ($106.80^\circ \pm 0.10^\circ$) with the smallest contact angles and DMSO ($123.00^\circ \pm 1.30^\circ$) in between. As shown before, all organic sample liquids show contact angles below 90° on a flat smooth PTFE foil and, as discussed, on graphite while organic liquids show contact angles larger than 90° on the GDL, which indicates a heterogeneous wetting phase for all organic solvents. With ongoing time all organic liquids slowly imbibe into the porous system. While the height of the DMSO droplet is nearly unchanged after 600 s, the width, measured at the solid liquid

interface, increases by 16% and the contact angle decreases to $108.40^\circ \pm 1.80^\circ$. This shows that DMSO only slightly penetrates into the porous system and shows, in principle, the usability of DMSO as solvent for electrolytes in Li–air batteries. Tetraglyme shows a decrease in height of the drop by around 14% and an increase of the width by 8%, accompanied by a decrease of the contact angle to $95.75^\circ \pm 0.75^\circ$. Compared to EC:DMC with a height decrease of 28%, a width decrease by 7% and a contact angle decrease to $82.25^\circ \pm 1.35^\circ$, this shows that Tetraglyme is already significantly wetting the porous system and therefore special treatment of the electrodes is necessary to allow the usage of Tetraglyme in Li–air batteries (**Table 2**).

2.2. Capillary Rise Measurement

The external contact angle, determined via goniometry describes the wettability of a liquid on a substrate, but gives no quantitative estimation for the wetting of a liquid into the porous electrode.

The driving force for liquid penetration into the porous system is the capillary pressure. The test liquid will rise inside the porous system until the capillary pressure and the hydrostatic pressure reach equilibrium. To measure these curves the setup shown in **Figure 8b** was used.

The measurement starts as soon as the GDL gets in contact with the sample liquid. During a short time, depending on the liquid properties, liquid not only imbibes into the porous system but a meniscus on the outside of the GDL is formed. As shown in **Figure 3**, all sample liquids show contact angles above 90° , leading to a nonwetting behavior and therefore to negative menisci for all sample liquids. This effect has the advantage, that meniscus formation could easily be subtracted from measured data, although some electrolyte might already penetrate the porous system. **Figure 4** shows the measured weight versus time curves, corrected for this meniscus formation.

Table 1. Calculated contact angles for sample liquids on PTFE foil and the GDL.

Sample liquid	Contact angle on PTFE [$^\circ$]	Contact angle on GDL at 0 s [$^\circ$]	Contact angle on GDL at 600 s [$^\circ$]
H_2O	109.05 ± 0.15	139.65 ± 0.35	133.30 ± 0.40
DMSO	75.40 ± 1.00	123.00 ± 1.30	108.40 ± 1.80
Tetraglyme	62.95 ± 0.35	106.80 ± 0.10	95.75 ± 0.75
EC:DMC	61.85 ± 0.65	105.15 ± 4.05	82.25 ± 1.35

Table 2. Calculated and measured values of sample liquid properties for capillary rise experiment and viscosity measurement (in bold) and literature values for surface tension and density.

Species	Volume μL [200 s]	Viscosity [mPa s]	Surface tension [mN m ⁻¹]	Density [g cm ⁻³]
H ₂ O	2.10 ± 0.57	0.934	72.75 ^[25]	1.00
DMSO	2.82 ± 0.64	2.251	43.54 ^[17]	1.10
Tetraglyme	2.02 ± 0.06	3.745	33.74 ^[26]	1.01
EC:DMC	4.73 ± 0.30	1.686	37.3 ^[27] ; 28.5 ^[28]	1.32 : 1.07

All sample liquids show very small liquid up-take over the measured time. While DMSO,^[29,30] H₂O^[31,32] and Tetraglyme,^[33,34] known solvents for Li-air batteries, show similar results, the Li-Ion reference solvent EC:DMC shows around 2 times higher uptake rates. Penetration of solvents into a porous structure is not solely dependent on contact angle but also on other parameters like viscosity. **Figure 5** shows measured viscosities for varying temperatures. Liquids with high viscosity take more time to rise than liquids with lower viscosities. While for water the high contact angle leads to nonwetting behavior with low uptake rates, Tetraglyme also shows low uptake rates although contact angles are smaller compared to water, due to a 4 times higher viscosity than H₂O (densities of H₂O and Tetraglyme are comparable, see Table 1). EC:DMC with a low viscosity and the smallest measured contact angle of all four sample liquids, shows the highest uptake rate which was more than two times higher than for H₂O. After an initial

fast solvent uptake, the rate slows down to a linear regime while all other three sample liquids show a linear uptake over the whole measurement time.

2.3. Capillary Pressure Measurement

While both measurements discussed above measure contact angles, pressure saturation curves provide a different access to the wetting properties of the sample liquids inside the porous system. To describe the porous system and the capillary pressure versus saturation relationship knowledge about negative and positive applied capillary pressures is mandatory. The capillary pressure is given as difference of the pressures in the liquid-phase and gas-phase.

$$P_c = P_L - P_G \quad (6)$$

with the liquid phase pressure P_L and the gas phase pressure P_G . The contact angle θ is linked to the capillary pressure with the Laplace equation shown in Equation (7) as simplified equation for a pipe with constant radius

$$P_c = \frac{4 \sigma \cos \theta}{d} \quad (7)$$

with the solid-liquid surface energy σ and the pore diameter d . Due to an averaging effect of the measurement, no locally

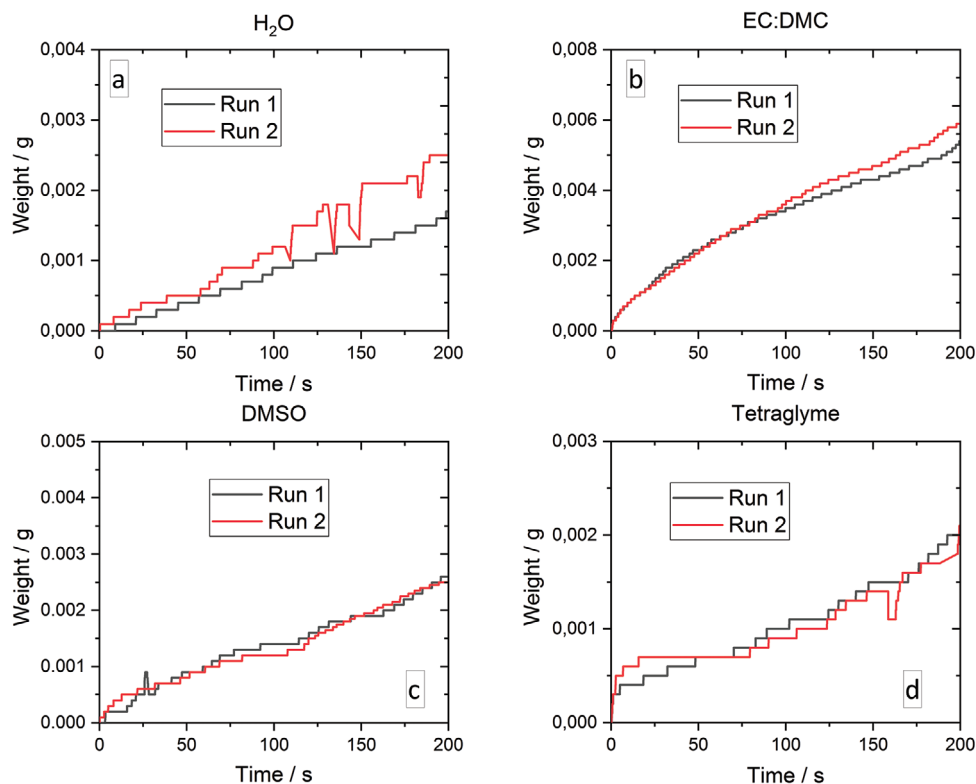


Figure 4. Recorded curves for capillary rise measurement of a) H₂O, b) EC:DMC, c) DMSO, and d) Tetraglyme. EC:DMC shows a slowing of uptake rate with time and a two times higher uptake rate compared to the other solvents. Water, Tetraglyme, and DMSO show an almost linear liquid uptake over time.

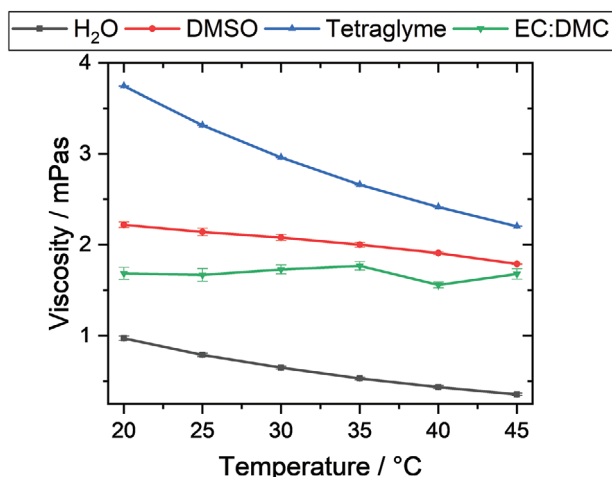


Figure 5. Viscosity for a temperature range from 20 to 45 °C, measured with 1 mL sample liquid at 100 Hz in a 0.5 mm slit between the 50 mm probe head and sample table.

resolved information can be obtained, therefore only averaged values for the contact angle can be determined. This technique allows for empirical analysis of porous media to predict the likelihood of flooding.^[35]

As described in literature^[12] and also shown in **Figure 6**, the first injection cycle shows higher capillary pressures for each saturation level, as also described by Harkness et al.^[35] This is due to the dry sample, with no residual H₂O inside. This residual water aids the water intrusion in later cycles and is the reason why the first two cycles in **Figure 6** show nonreproducible behavior in the high positive pressure regions. After these two cycles, reproducible behavior is observed; therefore, the third cycle will be used for comparison of different sample liquids as shown in **Figure 7**.

Figure 7a depicts curves for H₂O, EC:DMC, Tetraglyme, and DMSO. All values shown were normalized to the turnaround points of liquid injection and withdrawal described in the Experimental Section.

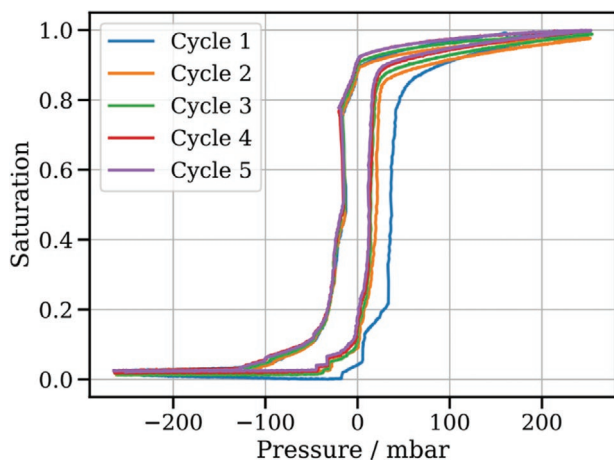


Figure 6. Five pressure saturation cycles of a Sigracet GDL 39BC with water. Blue shows the first imbibition, where higher capillary pressures are needed compared to all following cycles.

H₂O shows a well-known behavior reported in the literature.^[12–14] Starting from saturation point 0, filling of the porous system starts with negative capillary pressures until around 20% of the porous system is filled. The observation of negative capillary pressures is most probably due to residual water in some cavities and/or small crevices, which helps the reintroduction of water, while the main leg of water injection is at positive capillary pressures, indicating that the porous system is hydrophobic. At around 90% saturation level capillary pressure rises indicating that almost all pores are filled. Water begins to retract when negative capillary pressures are applied, following negative capillary pressure is observed over the whole water withdrawal process. When undergoing positive and negative capillary pressures, a hysteresis effect can be observed. While for the water intrusion regime the contact angle hysteresis is the main contributor to the capillary pressure hysteresis, for drainage it is reported to be pore size, shape and the surface structure.^[35] The surface structure properties differ inside the porous system due to nonisotropic distribution of PTFE and nonuniform surface structures.

For DMSO the high and low saturation levels do not show a slow start of imbibition or drainage like seen for water but a very defined start of both processes. Although DMSO is in the intermediate wetting regime, as shown before, it does not imbibe spontaneously into the porous system. Anderson observed that contact angles below 50° are necessary for spontaneous imbibition.^[36] It has been shown in the literature that wetting fluids still require positive pressures to enter the porous network.^[37,38] As additional feature DMSO shows higher capillary pressures during imbibition than water while having a lower contact angle. Since Tetraglyme showed a slower uptake rate at the capillary rise experiment while having a higher viscosity the changes in gas pressure are slow enough to allow for good distribution of DMSO inside the porous network and the higher pressures observed cannot be explained by viscosity effects. An explanation could be due to the applied negative pressure on gas side and the high melting point of DMSO of 18°C which may lead to the formation of metastable phases and therefore alter the contact angle, viscosity and surface tension. To verify this assumption temperature depended measurements would be necessary.

Like for H₂O a hysteresis effect occurs for DMSO, where the drainage starts at –330 mbar and is finished at –365 mbar. This stronger hysteresis, compared to water, might be due to stronger adsorption of DMSO onto the surface.

Tetraglyme shows negative pressures until a saturation of 60% is reached. Additionally, the measurement shows a slow start of imbibition as it was already observed for H₂O. Above 60%, saturation linearly increases up to 25 mbar at 100% saturation and pressure starts to increase strongly afterward. This shows that the porous system is completely filled, only trapped gas inside closed pores might be left. During withdrawal no changes in the saturation level can be observed until –180 mbar. Withdrawal of Tetraglyme appears abruptly since all liquid is withdrawn at –188 mbar.

EC:DMC shows a comparable trend to Tetraglyme during, imbibition the capillary pressure reaches only 2 mbar at 100% saturation, showing the higher tendency for wetting of this solvent mixture. Drainage shows a comparable trend as well between EC:DMC and Tetraglyme but drainage starts at –99 mbar for EC:DMC and ends at –108 mbar.

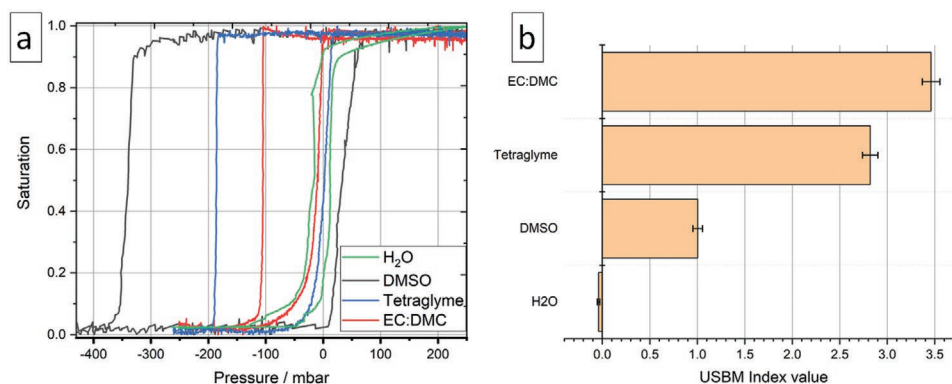


Figure 7. a) The third obtained pressure saturation curve for each solvent. b) The calculated USBM Index.

For better comparison of such experiments the US Bureau of Mines (USBM) wetting index is helpful, which is given by

$$I_{\text{USBM}} = \log\left(\frac{A_1}{A_2}\right) \quad (8)$$

where A_1 represents the area for negative capillary pressures and therefore the energy needed to withdraw liquid from the sample and A_2 the area for positive capillary pressures, which corresponds to the energy needed to imbibe liquid into the porous system.^[39] For water a value of I_{USBM} of -0.037 was calculated, indicating that nonwetting behavior of the porous system is dominating. DMSO gives an I_{USBM} of 1.004 , which means that DMSO wets the porous system, while Tetraglyme with an I_{USBM} of 2.820 and EC:DMC with 3.461 exceeding the value for DMSO showing the high wetting characteristics of both solvents.

3. Discussion

All experiments show the high wetting characteristics of the aprotic sample liquids. Although the contact angle

measurements on PTFE already showed contact angles in the wetting regime and additionally the test on GDL showed a penetration of the sample liquids inside the porous system, the actual wetted area inside the porous system depends on pore sizes and micro cavities of the particles within the porous network. Because this setup uses a horizontal probe table, the driving force for penetrating into the porous system is the capillary force acting against the gravitational force which makes a quantitative evaluation difficult. To test for the influence of capillary forces the capillary rise measurement was performed using the setup shown in **Figure 8b**. With this it could be shown that the penetration by capillary forces is highly influenced by the viscosity and surface tension.

While the lower contact angles aid the wetting of the porous media especially of small crevices and pores. Literature reports that BET surface does not necessarily correlate with capacity; as high BET surface carbons sometime show smaller capacities than low BET surface carbons.^[7] This is due to the low wettability of small pores, like sub micro pores and crevices. This low wettability also results in a lower active area. The lower active area also leads to reduced electrochemical performance since only wetted areas take part in the electrochemical reactions. In addition, in an actual Li–air battery the entrances to partially or

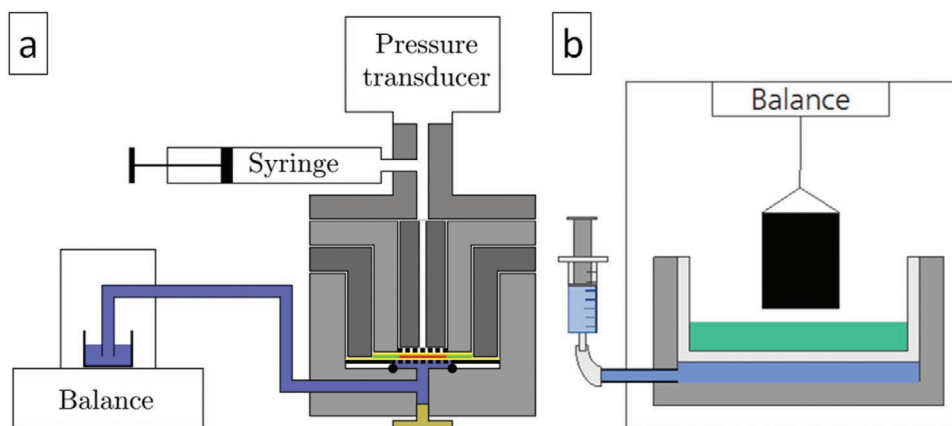


Figure 8. a) Pressure saturation setup. The saturation level is controlled by a syringe mounted into a syringe pump. The sample compartment consists of a hydrophilic membrane (yellow) between liquid compartment and sample (red) and a hydrophobic membrane (purple) between sample and atmosphere. b) Capillary rise setup, the height of the liquid container is changed by a syringe controlled liquid volume. Balance measures only the weight of sample and the sample holder.

fully flooded small crevices and pores are blocked by Li_2O_2 precipitates as Li_2O_2 forms favorable at the regions with higher gas concentrations^[7] which is near entrance to smaller pores due to the low oxygen diffusion. This would limit the mass-transfer of oxygen into the micro pore and therefore limit the specific capacity. The capillary rise experiments showed that high contact angles slow down the uptake rate of electrolyte. This helps to establish a stable triple phase boundary (which includes areas with ultrathin electrolyte film). In contrary small uptake rates due to high viscosity result in a continuous infinite flow of solvent into the porous system if no counterforce is present. During discharge of a Li-air battery Li_2O_2 is precipitated in the porous system, pushing electrolyte either out, and/or deeper into the porous system. If the solvent wets the cathode material, it will imbibe further into the porous system with each cycle due to the fact that it is more favorable to stay inside the porous system. This imbibition on the cathode side may lead to a dry out at the anode side of the battery and longer diffusion paths inside the porous system of the cathode from the electrolyte compartment to the active sites. As a consequence, low electrochemical performance is observed. Nonwetting properties of the solvent, on the other hand, are more favorable for the relaxation of solvent after precipitate dissolution.

Organic solvents are known for low polarity, which is one of the reasons for their superior wetting behavior.^[40,41] Identification of electrolytes with lower wettability and/or control of wetting inside the porous network would aid the development of a commercialization of Li-air batteries.

The electrolyte distribution inside the electrode for the different liquids determines the electrochemical performance, but heterogeneous distribution of electrolyte is quite complex and different effects alter this distribution like, e.g., microkinetics, electrowetting, or closed pores.^[42] The relation between the electrochemical performance and the wetting behavior is the ultimate goal which, however, requires operando structural and wetting behavior. The present study provides a step in this direction by addressing the properties of the different electrolyte solvents in the gas diffusion electrode. It has first to be considered that different viscosities result in different transport parameters, in particular the O_2 solubility is strongly depended on the solvent, second that the different wetting properties alter the gas-liquid interface with different overpotentials with varying electrowetting properties. Third, the precipitation of Li_2O_2 inside the porous system in Li- O_2 batteries is insulating and reduces the active area. For example, Gittleston et al. investigated the influence of different salts and oxygen diffusion coefficient in Tetraglyme and DMSO and showed variations in electrochemical performance which could not be attributed to the oxygen diffusion coefficient.^[43] They also showed lower discharge capacities in 1 M lithium bis(trifluoromethanesulfonyl) imide (LiTFSI)/Tetraglyme (0.18 mAh $\text{cm}^{-2}_{\text{ECSA}}$) than in 1 M LiTFSI/DMSO (0.087 mAh $\text{cm}^{-2}_{\text{ECSA}}$).

Franzen et al. investigated the influence of the electrolyte pressure onto the electrochemical performance showing that an intermediate electrolyte pressure results in the best performance.^[44] This finding is supported by Röhe et al. who modeled the influence of inhomogeneous electrolyte distribution in silver based GDEs and showed that it is highly desirable to reduce electrolyte intrusion since the performance can be

attributed to a large active gas-liquid interface which is located near the electrolyte bulk to reduce mass transport limitations.^[45] This might be due to the different transport parameters of O_2 in the gas phase ($D = 0.1 \text{ cm}^2 \text{ s}^{-1}$ ^[46]) and the electrolyte (water: $2.3 \times 10^{-5} \text{ cm}^2 \text{ s}^{-1}$,^[47] 1 M LiTFSI/DMSO: $1.28 \times 10^{-5} \text{ cm}^2 \text{ s}^{-1}$ ^[43] and 1 M LiTFSI/Tetraglyme: $1.60 \times 10^{-7} \text{ cm}^2 \text{ s}^{-1}$ ^[43]) as well as the slower ionic transport of Li^+ . Schröder et al. showed the influence by comparing a split GDL and showed that the section without PTFE treatment showed lower performance with around 125 mA cm^{-2} than the one treated with PTFE with around 175 mA cm^{-2} and explains it with the higher water saturation of the untreated GDL.^[42] Paulisch et al. showed that electrolyte flooding starts at larger pore channels and allow for percolation through the GDE.^[48]

An optimal electrode structure would be built by a gradient in the pore size distribution with larger pores at the gas side and smaller pores at the electrolyte bulk. Smaller pores have a higher capillary pressure (p_1) and are filled with electrolyte, the larger pores have lower capillary pressures (p_2). By setting the gas pressure between p_1 and p_2 the electrolyte saturation can be adjusted to be only in the region with smaller pores. This electrode design is known from alkaline fuel cell and called double skeleton electrode.^[49] By treating the larger pores with a nonwetting binder or surface layer the capillary pressure p_2 can be reduced even further, increasing the effect of gas filled pores and enables gas transport to the active sides for a wider operation window.

In our study it can be shown that the results of DMSO, used for GDEs which were optimized for the operation with aqueous electrolytes, cannot be used at their full potential. But both, the contact angle measurement over time and the pressure saturation curves showed that DMSO only slightly penetrates into the porous network. For Tetraglyme this is not the case, since it is wetting the cathode materials more than DMSO as was shown by using the USBM Index and contact angle over time measurements. Strategies for the usage of organic electrolytes, beside the ones pointed out above, have to be identified to achieve high cycle life, rate capability and capacity.

Several approaches would be possible to control the surface wetting inside the porous system and therefore optimize the electrodes for organic electrolytes. One approach would be to use mixtures of hydrophilic organics with water to increase the surface tension,^[50] and lower the viscosity.^[51] This approach is already investigated for Zn-air batteries, where the anode does not need special protection against water.^[52] For Li-air batteries special water inhibiting separators would be needed, since most solid electrolytes are still porous, water diffusion may not be blocked completely, and by that reducing the cycle life. Another possible option for better control of the wetting behavior inside the porous system would be the usage of nonwetttable binders, but they have to be chosen carefully since some binders dissolve in some electrolyte solvents, like polyvinylidene fluoride in DMSO.^[53] With nonwetting binders a fuel cell-like electrode could be produced, where hydrophilic and hydrophobic pores control the penetration of electrolyte into the porous system. This approach could also be achieved by applying the treatment used for the PTFE membrane inside the pressure saturation curve setup in this work.

Another possibility would be a continuous gas-diffusion network within the porous system, to enhance oxygen transport

through the whole electrode.^[5,54] To achieve this, it would be favorable to wet the whole GDE substrate with a very thin liquid film obtaining high wetted surfaces and therefore high capacities and at the same time avoid gas transport limitations, which would require high ionic conductivity of the electrolyte because the small area for ionic transport in the thin electrolyte films. If ionic conductivity is too low reactants cannot reach the whole wetted area resulting in loss of active area during continuous operation due to transport limitations.

As reported in literature, capacity is depending on the saturation level and therefore wetted surface inside the porous system. For classical systems where electrolyte fills pore volume completely, capacity rises with increase of electrolyte volume due to increase of diffusion paths and therefore higher effective ionic diffusivity, while at a certain point flooding of the electrode occurs, which results in a blockage of the oxygen supply.^[55] For systems with a thin wetting film throughout the porous network, oxygen only has to diffuse through this thin layer and not through a blocking flooded system avoiding mass transport limitations. One possibility would be to use a high wetting solvent and the usage of pressurized gas to avoid flooding of the electrode. But this would work solely for horizontal build Li-air batteries; as soon as the battery is tilted pressurized gas will not be able to stop flooding of the lower part of the porous system and might even increase flooding.

The most favorable way would be the usage of an artificial three-phase reaction zone, which would help avoid flooding of the whole porous network and furthermore could be designed to withhold water, improving the cycle life and avoiding unwanted side reactions. One attempt to create an artificial triple phase zone was already performed by Balaish et al., using perfluorinated carbon liquids.^[56]

Another aspect to be kept in mind is the influence of electrolyte salts, which was not investigated in this work but will alter the wetting behavior of the electrolyte, e.g., water with dissolved salt shows a higher surface tension due to repulsion of ions from the surface by the electrostatic force.^[57]

4. Conclusion

The wetting behavior of pure Tetraglyme and DMSO were compared to the wetting behavior of H₂O and a 1:1 volume fraction mixture of EC:DMC for a Sigracet 39BC GDL. EC:DMC was used as reference point for a wetting fluid, while water was used as reference point for a nonwetting fluid. It could be shown that all three organic based solvents wet the GDL. While DMSO still is in the intermediate wetting regime with a contact angle of 72° on PTFE, Tetraglyme is already in the wetting regime with a contact angle of 62° on PTFE. This is comparable to the EC:DMC mixture with a contact angle of 60° on PTFE. Contact angle measurements for a Sigracet 39BC GDL showed a slow penetration of all organic liquids into the porous network. Comparison of liquid absorption rates with the capillary rise method showed that flow rate of organic solvents is mainly depending on the viscosity, which led to comparable uptake rates of nonwetting water ($2.10 \pm 0.57 \mu\text{L}/200 \text{ s}$) and highly wetting Tetraglyme ($2.02 \pm 0.06 \mu\text{L}/200 \text{ s}$), but with different limiting factors. The flow rate of Tetraglyme is believed

to be limited by the high viscosity (3.745 mPa s), while the water uptake rate is believed to be limited by the hydrophobic properties of the GDL. To verify the wetting behavior of the organic liquids, pressure saturation measurements were performed, unveiling that EC:DMC and Tetraglyme are highly wetting the GDL used here. On the other hand, DMSO required higher capillary pressures for imbibition compared to water although having a lower contact angle. One explanation might be the formation of metastable phases of DMSO through to the high melting point of 18°C and the used wide pressure range during pressure saturation curve recording. This phenomenon could not be explained properly since no temperature depended measurements could be performed. The pressure saturation curve obtained for water were similar to results shown in literature. Because all organics imbibed the porous network containing PTFE, cathode flooding with these electrolytes might occur and ultimately results in a small active area. This will lead to lower rate capabilities and lower cycle life due to higher over potentials and therefore the electrolyte might decompose faster.

5. Experimental Section

The wetting behavior of four different solvents, DMSO (VWR Chemicals), Tetraglyme (Merck), EC (anhydrous 99%), and DMC ($\geq 99\%$), was studied for a Sigracet GDL 39BC. Sigracet 39BC is a nonwoven carbon paper gas diffusion media with a microporous layer (MPL) and a total thickness of 325 μm (microns). It was PTFE treated to 5 wt%. EC and DMC were mixed in a 1:1 volume fraction, after liquefying DMC at 40 °C, this mixture will be called EC:DMC in the following. The wetting behavior of the pure solvents and EC:DMC was compared to the wetting behavior of H₂O (Water Alfa Aesar ultrapure HPLC grade) for a 39BC GDL. Beside water as a reference point for nonwetting solvent on PTFE, EC:DMC was used as reference point for a PTFE wetting liquid.

To characterize the wetting behavior of these sample liquids, the following three measurement techniques were used, each unveiling different properties of the wetting behavior.

Contact angle measurements were performed with a homemade setup, consisting of a Visicom CCD-BW7212 1/2" camera, a Leitz 100 W lamp (type 307-107.003), and EM12 V2.3 software (Hesse Instruments). The contact angle was measured between solvent drops and the surface of a PTFE foil (BOLA, 0.5 mm) or the GDL. Each substrate was glued with a double-sided adhesive tape to a flat surface. A 15 μL drop of liquid was placed onto the surface prior to the measurement. For the GDL, pictures were taken in a 10 s interval for 20 min. The contact angle was calculated with ImageJ and the plugin contact angle.

Capillary rise experiments were taken using a setup shown in Figure 8, which was installed into an OHAUS Adventurer AX324 balance. To avoid changes in the height of liquid while liquid was imbibed into the sample and diminish influences of changing amounts of sample liquid vapor phase onto the measurement, the liquid filled container was placed into a sealed compartment for 10 min, after the sample was mounted onto the holder, data recording was started. The container was then lifted with a syringe until the sample touched the liquid surface. The mass increase was recorded for 300 s and corrected for meniscus formation during first contact between sample and liquid.

Pressure saturation curves were recorded using a homemade cell, shown in Figure 8, with a pressure transducer (DMP 311 from BD sensors, $\pm 0.5 \text{ bar}$, $\pm 0.1\%$) which was monitored with a data logger (Agilent 34970A Data Acquisition). The syringe (Hamilton 1001TLL 1.0 mL) was controlled with a syringe pump (NE-500). All used liquids were degassed with a vacuum pump and the channels of the cell were scoured with these solvents until no gas was left in the liquid compartment. After sealing the liquid compartment with a hydrophilic membrane (Merck Durapore Membrane Filter 0.45 μm HV) a negative pressure of

–300 mbar was applied at the liquid container placed in the balance and maintained during assembly. After a short waiting period to achieve pressure equilibrium inside the system the sample was pressed inside a PTFE ring and mounted with an omniphobic membrane (Whatman Membrane Filter 0.2 μm WTP Type treated with FluoroPel 800 2%) on top of it. The other cell parts were connected and fixed with screws.

The measurement consisted of cycles between the two selected turning pressures (± 500 mbar for DMSO and ± 250 mbar for H_2O , Tetraglyme and EC:DMC). The pressure was changed linear until one of the two turn around pressures for withdrawal or injection was reached. At these points the direction of the syringe pump was reverted. Each measurement consisted of 5 cycles, to assure reproducible cycles.

A Rheometer (Anton Paar Physica MCR 101) with a 50 mm probe head (Anton Paar Pp50, Diameter 50 mm) was used to measure the viscosity. For this, 1 mL was placed in a 0.5 mm slit between the probe head and the probe table and the probe head was rotated with a fixed rotation speed of 100 Hz. For each temperature (20–45 $^{\circ}\text{C}$, in 5 $^{\circ}\text{C}$ steps), 10 measurements were taken.

Acknowledgements

The authors specially thank the German ministry BMBF for funding this work with the project LiBaLu (FKZ.: 03XP0029C), Linus Kube and Christina Schmitt for their experimental support and fruitful discussions, and Werner Seybold for maintaining and modifying the test setups.

Open access funding enabled and organized by Projekt DEAL.

Conflict of Interest

The authors declare no conflict of interest.

Data Availability Statement

The data that support the findings of this study are available from the corresponding author upon reasonable request.

Keywords

contact angle, Li–air battery, organic solvents, pressure saturation curves, wettability

Received: August 20, 2021

Revised: November 10, 2021

Published online:

- [1] J. W. Choi, D. Aurbach, *Nat. Rev. Mater.* **2016**, 1, 16013.
- [2] F. Bidault, D. J. L. Brett, P. H. Middleton, N. P. Brandon, *J. Power Sources* **2009**, 187, 39.
- [3] X. Li, H. K. Lee, I. Y. Phang, C. K. Lee, X. Y. Ling, *Anal. Chem.* **2014**, 86, 10437.
- [4] N. Wagner, M. Schulze, E. Gülzow, *J. Power Sources* **2004**, 127, 264.
- [5] C. Xia, C. L. Bender, B. Bergner, K. Peppeler, J. Janek, *Electrochem. Commun.* **2013**, 26, 93.
- [6] P. Andrei, J. P. Zheng, M. Hendrickson, E. J. Plichta, *J. Electrochem. Soc.* **2010**, 157, A1287.
- [7] J. Read, *J. Electrochem. Soc.* **2002**, 149, A1190.
- [8] E. Chibowski, L. Holysz, *J. Adhes. Sci. Technol.* **1997**, 11, 1289.
- [9] E. Chibowski, R. Perea-Carpio, *Adv. Colloid Interface Sci.* **2002**, 98, 245.

- [10] H. Czachor, *Process* **2007**, 21, 2239.
- [11] J. Tröger, K. Lunkwitz, K. Grundke, W. Bürger, *Colloids Surf., A* **1998**, 134, 299.
- [12] J. D. Fairweather, P. Cheung, J. St-Pierre, D. T. Schwartz, *Electrochem. Commun.* **2007**, 9, 2340.
- [13] J. T. Gostick, M. A. Ioannidis, M. W. Fowler, M. D. Pritzker, *Electrochem. Commun.* **2008**, 10, 1520.
- [14] T. V. Nguyen, G. Lin, H. Ohn, X. Wang, *Electrochem. Solid-State Lett.* **2008**, 11, B127.
- [15] E. Dujardin, T. W. Ebbesen, H. Hiura, K. Tanigaki, *Science* **1994**, 265, 1850.
- [16] Y. Wei, Q. Zhang, J. E. Thompson, *Atmos. Clim. Sci.* **2017**, 7, 11.
- [17] A. P. G. Arthur, W. Adamson, *Physical Chemistry of Surfaces*, John Wiley & Sons Inc, New York **1997**.
- [18] F. Taherian, V. Marcon, N. F. A. van der Vegt, F. Leroy, *Langmuir* **2013**, 29, 1457.
- [19] D. Bevers, R. Rogers, M. von Bradke, *J. Power Sources* **1996**, 63, 193.
- [20] S. Goswami, S. Klaus, J. Benziger, *Langmuir* **2008**, 24, 8627.
- [21] M. Yekta-Fard, A. B. Ponter, *J. Colloid Interface Sci.* **1988**, 126, 134.
- [22] K. Grundke, T. Bogumil, T. Gietzelt, H. J. Jacobasch, D. Y. Kwok, A. W. Neumann, in *Interfaces, Surfactants and Colloids in Engineering*, Vol. 101 (Ed: H. J. Jacobasch), Steinkopff, Darmstadt, Germany **1996**, Ch. 11.
- [23] G. Wolansky, A. Marmur, *Colloids Surf., A* **1999**, 156, 381.
- [24] A. J. B. Milne, A. Amirfazli, *Adv. Colloid Interface Sci.* **2012**, 170, 48.
- [25] N. B. Vargaftik, B. N. Volkov, L. D. Voljak, *J. Phys. Chem. Ref. Data* **1983**, 12, 817.
- [26] S. K. Begum, R. J. Clarke, M. S. Ahmed, S. Begum, M. A. Saleh, *J. Mol. Liq.* **2013**, 177, 11.
- [27] C. Wohlfarth, in *Landolt-Börnstein IV/24: Surface Tension of Pure Liquids and Binary Liquid Mixtures*, Vol. 24 (Eds: M. D. Lechner), Springer, Berlin, Germany **2008**, Ch. p. 42.
- [28] F. Wang, J. Wu, Z. Liu, *Fluid Phase Equilib.* **2004**, 220, 123.
- [29] N. Mozhzhukhina, L. P. Méndez De Leo, E. J. Calvo, *J. Phys. Chem. C* **2013**, 117, 18375.
- [30] M. J. Trahan, S. Mukerjee, E. J. Plichta, M. A. Hendrickson, K. M. Abraham, *J. Electrochem. Soc.* **2012**, 160, A259.
- [31] B. M. Gallant, *Joule* **2020**, 4, 2254.
- [32] D. Wittmaier, S. Aisenbrey, N. Wagner, K. A. Friedrich, *Electrochim. Acta* **2014**, 149, 355.
- [33] M. Marinaro, S. Theil, L. Jörissen, M. Wohlfahrt-Mehrens, *Electrochim. Acta* **2013**, 108, 795.
- [34] Q. Zhao, Y. Zhang, G. Sun, L. Cong, L. Sun, H. Xie, J. Liu, *ACS Appl. Mater. Interfaces* **2018**, 10, 26312.
- [35] I. R. Harkness, N. Hussain, L. Smith, J. D. B. Sharman, *J. Power Sources* **2009**, 193, 122.
- [36] W. G. Anderson, *J. Pet. Technol.* **1987**, 39, 1283.
- [37] B.-S. Kim, P. Harriott, *J. Colloid Interface Sci.* **1987**, 115, 1.
- [38] W. R. Purcell, *J. Pet. Technol.* **1949**, 1, 39.
- [39] J. T. Gostick, M. A. Ioannidis, M. W. Fowler, M. D. Pritzker, *J. Power Sources* **2009**, 194, 433.
- [40] J.-S. Lee, S. T. Kim, R. Cao, N.-S. Choi, M. Liu, K. T. Lee, J. Cho, *Adv. Energy Mater.* **2011**, 1, 34.
- [41] M. M. Pereira, K. A. Kurnia, F. L. Sousa, N. J. O. Silva, J. A. Lopes-da-Silva, J. A. P. Coutinho, M. G. Freire, *Phys. Chem. Chem. Phys.* **2015**, 17, 31653.
- [42] A. Schröder, K. Wippermann, W. Lehnert, D. Stolten, T. Sanders, T. Baumhöfer, N. Kardjilov, A. Hilger, J. Banhart, I. Manke, *J. Power Sources* **2010**, 195, 4765.
- [43] F. S. Gittleston, R. E. Jones, D. K. Ward, M. E. Foster, *Energy Environ. Sci.* **2017**, 10, 1167.
- [44] D. Franzen, B. Ellendorff, M. C. Paulisch, A. Hilger, M. Osenberg, I. Manke, T. Turek, *J. Appl. Electrochem.* **2019**, 49, 705.
- [45] M. Röhe, D. Franzen, F. Kubannek, B. Ellendorff, T. Turek, U. Krewer, *Electrochim. Acta* **2021**, 389, 138693.

- [46] Y. Bultel, K. Wiezell, F. Jaouen, P. Ozil, G. Lindbergh, *Electrochim. Acta* **2005**, 51, 474.
- [47] W. Xing, M. Yin, Q. Lv, Y. Hu, C. Liu, J. Zhang, in *Rotating Electrode Methods and Oxygen Reduction Electrocatalysts*, (Eds: W. Xing, G. Yin, J. Zhang) Elsevier, Amsterdam, the Netherland **2014**, Ch. 1.
- [48] M. C. Paulisch, M. Gebhard, D. Franzen, A. Hilger, M. Osenberg, N. Kardjilov, B. Ellendorff, T. Turek, C. Roth, I. Manke, *Materials* **2019**, 12, 2686.
- [49] K. J. Euler, *Chem. Unserer Zeit* **1967**, 1, 9.
- [50] W. Martino, J. F. de la Mora, Y. Yoshida, G. Saito, J. Wilkes, *Green Chem.* **2006**, 8, 390.
- [51] K. R. Seddon, A. Stark, M.-J. Torres, *Pure appl. Chem.* **2000**, 72, 2275.
- [52] Z. Liu, S. Z. E. Abedin, F. Endres, *Electrochim. Acta* **2013**, 89, 635.
- [53] A. Bottino, G. Capannelli, S. Munari, A. Turturro, *J. Polym. Sci., Part B: Polym. Phys.* **1988**, 26, 785.
- [54] W. Xu, J. Xiao, J. Zhang, D. Wang, J.-G. Zhang, *J. Electrochem. Soc.* **2009**, 156, A773.
- [55] J. Christensen, P. Albertus, R. S. Sanchez-Carrera, T. Lohmann, B. Kozinsky, R. Liedtke, J. Ahmed, A. Kojic, *J. Electrochem. Soc.* **2011**, 159, R1.
- [56] M. Balaish, A. Kraytsberg, Y. Ein-Eli, *ChemElectroChem* **2014**, 1, 90.
- [57] L. Onsager, N. N. T. Samaras, *J. Chem. Phys.* **1934**, 2, 528.